

# Metal Donor $\rightarrow$ Metal Acceptor Complexes: $\text{Fe}(\text{CO})_4^{2-}$ , $\text{HFe}(\text{CO})_4^-$ , and $\text{trans-HFe}(\text{CO})_3\text{P}(\text{OMe})_3^-$ as Anionic Ligands to $\text{M}(\text{CO})_5^0$ , $\text{M} = \text{Cr}, \text{W}^\dagger$

Larry W. Arndt, Marcetta Y. Darensbourg,\* Terry Delord, and Barbara Trzcinska Bancroft

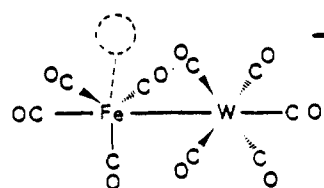
Contribution from the Department of Chemistry, Texas A&M University, College Station, Texas 77843. Received October 16, 1985

**Abstract:** A series of heterobimetallic carbonyl anions have been synthesized and structurally characterized as their bis-(triphenylphosphine)iminium salts. Compound 1,  $\text{PPN}^+\text{HFeW}(\text{CO})_9^-$ , crystallizes in space group  $P\bar{1}$  ( $Z = 2$ ):  $a = 14.099$  (5) Å,  $b = 11.601$  (5) Å,  $c = 14.148$  (5) Å,  $\alpha = 95.53$  (3)°,  $\beta = 118.23$  (3)°,  $\gamma = 92.39$  (3)°,  $V = 2026$  (3) Å<sup>3</sup>;  $R_w = 0.061$  for 3637 unique reflections measured  $>3\sigma(I)$ . Compound 2,  $\text{PPN}^+\text{HFeW}(\text{CO})_8\text{P}(\text{OMe})_3^-$ , crystallizes in space group  $P2_1/N$  ( $Z = 4$ ):  $a = 12.200$  (2) Å,  $b = 12.461$  (2) Å,  $c = 32.032$  (4) Å,  $\alpha = 90.00^\circ$ ,  $\beta = 96.40$  (1)°,  $\gamma = 90.00^\circ$ ,  $V = 4838$  (2) Å<sup>3</sup>;  $R_w = 0.069$  for 1769 unique reflections measured  $>3\sigma(I)$ . Compound 3,  $\text{PPN}^+\text{HFeCr}(\text{CO})_9^-$ , crystallizes in space group  $P\bar{1}$  ( $Z = 2$ ):  $a = 11.717$  (2) Å,  $b = 14.095$  (3) Å,  $c = 14.283$  (2) Å,  $\alpha = 92.18$  (2)°,  $\beta = 117.51$  (1)°,  $\gamma = 95.78$  (2)°,  $V = 2072$  (1) Å<sup>3</sup>;  $R_w = 0.053$  for 1321 unique reflections measured  $>3\sigma(I)$ . Finally, compound 4,  $(\text{PPN}^+)_2\text{FeCr}(\text{CO})_9^{2-}$ , crystallizes in space group  $P\bar{1}$  ( $Z = 2$ ):  $a = 13.882$  (2) Å,  $b = 22.825$  (4) Å,  $c = 13.067$  (2) Å,  $\alpha = 96.07$  (1)°,  $\beta = 117.57$  (1)°,  $\gamma = 87.27$  (1)°,  $V = 3650$  (2) Å<sup>3</sup>;  $R_w = 0.060$  for 3905 unique reflections measured  $>3\sigma(I)$ . The structural features common to all complexes are all terminal CO groups and a Fe-M ( $\text{M} = \text{Cr}, \text{W}$ ) bond. This bond is viewed as a Fe:  $\rightarrow$  M donor-acceptor complex in which Fe<sup>2+</sup> donates to an electrophilic group 6 metal pentacarbonyl moiety. In the series, the Fe-M bond distance ranges from 2.941 (2) Å for 4 to 2.997 (2) Å for 1. The small bond distance change of 0.015 Å on going from the dianion 4 to the protonated form 3 and the appropriate  $(\text{OC})_{\text{eq}}\text{-Fe}(\text{CO})_{\text{eq}}$  angle deformations as well as the identical M-CO arrangement of the  $\text{Ph}_3\text{PAuFeW}(\text{CO})_9^-$  anion suggest the hydride to be terminal and located solely on Fe. Various spectral (IR, <sup>13</sup>C NMR) and chemical characterizations are also reported.

The chemistry of mixed metal binuclear complexes is a rapidly developing area of inorganic/organometallic chemistry.<sup>1,2</sup> The extent to which the M-M' bond might be described as a donor-acceptor or dative bond, i.e.,  $\text{M} \rightarrow \text{M}'$ ,<sup>3</sup> may be addressed in terms of reactivity, structure, and theory. For example, if the "18-electron-complex ligand"<sup>3d</sup>  $\text{L}_n\text{M}$ : behaves as an innocent ligand, ligand lability studies might be designed to relate the donor complex to more common ligands such as P-, N-, S-, or O-donor ligands, halides, or CO. Furthermore it is expected that the donor ability of M: might be tailored by ancillary ligand modification. Problems of inter- and intramolecular ligand mobility, and competitive M:  $\rightarrow$  M' bond disruption, are expected to be influenced by the intrinsic polarity or electron drain/gain, of the M:  $\rightarrow$  M' bond.

We have recently isolated a series of anionic heterobinuclear complexes which are being used to address some of these questions as well as to gain synthetic entry into derivatized mixed metal complexes. Herein we report X-ray crystal structure determinations of four members of this series: the bis(triphenylphosphine)iminium,  $\text{PPN}^+$ , salts of  $\text{HFeW}(\text{CO})_9^-$  (1), a phosphite-substituted analogue,  $\text{HFeW}(\text{CO})_8\text{P}(\text{OMe})_3^-$  (2),  $\text{HFeCr}(\text{CO})_9^-$  (3), and its conjugate base  $\text{FeCr}(\text{CO})_9^{2-}$  (4). A preliminary report of one of these,  $\text{PPN}^+\text{HFeW}(\text{CO})_9^-$ , indicated the elementary nature of the complex hydrides: there is a metal-metal bond, the coordination geometry about W is octahedral, and the Fe might be described as a doubly perturbed tetrahedron or a very distorted octahedron.<sup>4</sup> Although the hydride ligand could not be located in the X-ray structure analysis, ab initio calculations have optimized its position solely on Fe,<sup>5</sup> as indicated in the stick drawing. These calculations have as well defined the character of the mixed metal bond.<sup>5</sup>

Further evidence for the position of the hydride as a terminal ligand on Fe was found in the X-ray structure determination of  $\text{Et}_4\text{N}^+\text{Ph}_3\text{PAuFeW}(\text{CO})_9^-$ , 5.<sup>6</sup> This heterotrimetallic anion,



prepared by the addition of  $\text{Ph}_3\text{PAuCl}$  to  $\text{FeW}(\text{CO})_9^{2-}$ , showed a metal carbonyl arrangement practically identical with 1 and the  $\text{Ph}_3\text{Au}$  located solely on Fe. The structure of this anion will be compared with anions 1-4 below.

Both the Fe and the group 6 metal centers may be modified by substitution of CO ligands by P-donor ligands. We have done this and report as well on ligand effects in the description of the Fe  $\rightarrow$  M bond as a Lewis acid-base interaction. The utility of certain members of this series as olefin isomerization catalysts is the subject of a separate report.<sup>7</sup>

## Experimental Section

**General Procedures.** All operations are carried out under nitrogen using standard Schlenk techniques or in an argon atmosphere glovebox. Solvents were dried and degassed as described below. Infrared spectra were recorded on a Perkin-Elmer 283 spectrophotometer for routine runs, and detailed spectra were obtained on an IBM FT/85 spectrophotometer

(1) Roberts, D. A.; Geoffroy, G. L. In *Comprehensive Organometallic Chemistry*; Wilkinson, G., Ed.; Pergamon: Oxford, 1982; Vol. 6, pp 763-877 and references therein.

(2) (a) Casey, C. P.; Bullock, R. M. *Organometallics* 1984, 3, 1100. (b) Mercer, W. C.; Whittle, R. R.; Burkhardt, E. W.; Geoffroy, G. L. *Organometallics* 1985, 4, 68. (c) Casey, C. P.; Bullock, R. M. *J. Mol. Catal.* 1982, 14, 283.

(3) (a) Anders, U.; Graham, W. A. G. *J. Am. Chem. Soc.* 1967, 89, 539. (b) Einstein, F. W. B.; Pomeroy, R. K.; Rushman, P.; Willis, A. C. *Organometallics* 1985, 4, 250. (c) Einstein, F. W. B.; Jones, T.; Pomeroy, R. K.; Rushman, P. *J. Am. Chem. Soc.* 1984, 106, 2707. (d) Einstein, F. W. B.; Pomeroy, R. K.; Rushman, P.; Willis, A. C. *J. Chem. Soc., Chem. Commun.* 1983, 854. (e) Chin, H. B.; Smith, M. B.; Wilson, R. D.; Bau, R. *J. Am. Chem. Soc.* 1974, 96, 5285.

(4) Arndt, L. W.; Delord, T.; Darensbourg, M. Y. *J. Am. Chem. Soc.* 1984, 106, 456.

(5) Hall, M. B.; Halpin, C. *J. Am. Chem. Soc.*, in press.

(6) Arndt, L. W.; Darensbourg, M. Y.; Fackler, J. P.; Lusk, R. J.; Marler, D. O.; Youngdahl, K. A. *J. Am. Chem. Soc.* 1985, 107, 7218.

(7) Tooley, P. A.; Arndt, L. W.; Darensbourg, M. Y. *J. Am. Chem. Soc.* 1985, 107, 2422.

<sup>†</sup> In this paper the periodic group notation in parentheses is in accord with recent actions by IUPAC and ACS nomenclature committees. A and B notation is eliminated because of wide confusion. Groups IA and IIA become groups 1 and 2. The d-transition elements comprise groups 3 through 12, and the p-block elements comprise groups 13 through 18. (Note that the former Raman number designation is preserved in the last digit of the numbering: e.g., III  $\rightarrow$  3 and 13.)

Table I. Spectral Properties:  $^1\text{H}$  NMR and Infrared THF Solution Spectra

class	anion	$^1\text{H}$ NMR, ppm	$J_{(\text{P-H})}$ , Hz	$J_{(\text{W-H})}$ , Hz	IR $\nu(\text{CO})$ , $\text{cm}^{-1}$	
					major	others
I	$\text{HFeM}(\text{CO})_5^-$					
	M = Cr	-13.4			1942 s	2057 vw, 2012 w, 2000 m, 1911 m, 1880 m
	M = W	-11.8		15.0	1940 s	2063 vw, 2009 m, 1911 m, 1870 m
II	$\text{P}(\text{CO})_3\text{HFeM}(\text{CO})_5^-$					
	M = Cr; P = $\text{PPh}_3$	-13.0	24.7		1923 s	2048 w, 2030 m, 1956 w, 1894 m, 1873 w, 1869 sh
	M = Cr; P = $\text{P}(\text{OMe})_3$	-15.3	22.5		1929 s	2050 vw, 2035 w, 1956 w, 1897 m, 1870 m, 1851 sh
	M = W; P = $\text{PPh}_3$	-11.8	24.7	9.5	1928 s	2060 w, 2046 w, 1960 w, 1900 m, 1847 w, br
	M = W; P = $\text{PMe}_3$	-12.6	26.3	14.3	1918 s	2053 w, 2039 w, 1888 m, 1842 m, br
	M = W; P = $\text{PET}_3$	-12.5	27.0	11.0	1918 s	2054 w, 2040 m, 1889 m, 1843 m, br
	M = W; P = $\text{P}(\text{OMe})_3$	-12.8	22.6	16.6	1927 s	2059 w, 2046 w, 1964 w, 1901 w, 1864 m
	M = W; P = $\text{P}(\text{OEt})_3$	-12.9	20.4	18.0	1926 s	2059 w, 2045 w, 1963 w, 1900 w, 1863 m, br
III	$(\text{CO})_4\text{FeHW}(\text{CO})_4\text{P}^-$					
	P = $\text{PPh}_3$	-13.4	23.1	33.0	1921 s	2028 m, 1996 m, 1893 w, 1873 w, 1843 m, br
	P = $\text{P}(\text{OMe})_3$	-14.4	27.0	28.5	1924 s	2033 w, 1999 m, 1882 m, 1838 m, br
IV	$\text{FeM}(\text{CO})_9^-$					
	M = Cr				1892 s	2009 w, 1907 w, sh, 1814 m
	M = W				1899 s	2026 w, 1808 m

Table II.  $^{13}\text{C}$  NMR Resonances, Referenced to  $\text{Me}_4\text{Si}$ 

salt	temp/solvent	$\text{Fe}(\text{CO})_4$ , ppm	$\text{M}(\text{CO})_{\text{ax}}$ , ppm	$\text{M}(\text{CO})_{\text{eq}}$ , ppm
$(\text{Et}_4\text{N}^+)_2\text{FeW}(\text{CO})_9^-$	-50 °C/THF + $\text{CH}_3\text{CN}$	224.8	213.7	213.5 ( $J_{\text{W-C}} = 125.5$ Hz)
$(\text{Et}_4\text{N}^+)_2\text{FeCr}(\text{CO})_9^-$	-70 °C/THF + $\text{CH}_3\text{CN}$	225.3	238.0	233.9
$\text{PPN}^+\text{HFeW}(\text{CO})_9^-$	23 °C/ $\text{CH}_3\text{CN}$	218.1	203.9	203.0 ( $J_{\text{W-C}} = 125.6$ Hz)
$\text{PPN}^+\text{HFe}(\text{CO})_3(\text{P}(\text{OMe})_3)\text{W}(\text{CO})_5^-$	23 °C/ $\text{CH}_3\text{CN}$	218.5	204.9	204.1 ( $J_{\text{W-C}} = 125.6$ Hz)

using 0.10-mm  $\text{CaF}_2$  cells. Proton NMR spectra were measured on a 90-MHz Varian EM390, and  $^{31}\text{P}$  and  $^{13}\text{C}$  NMR spectra were recorded on a XL200 Varian spectrometer.  $^{31}\text{P}$ ,  $^{13}\text{C}$ , and  $^1\text{H}$  NMR spectra were referenced against  $\text{H}_3\text{PO}_4$ , benzene- $d_6$ , and THF, respectively. Benzene and THF were ultimately referenced against  $\text{Me}_4\text{Si}$ .

**Materials.** Tetrahydrofuran (THF) and hexane were distilled under nitrogen from sodium/benzophenone. Acetone was dried over calcium hydride and stored under nitrogen over 3-Å molecular sieves. Diethyl ether was freshly distilled from lithium aluminum hydride.  $\text{PPN}^+$  or  $\text{Et}_4\text{N}^+$  salts of  $\text{HFe}(\text{CO})_4^-$  and *trans*- $\text{HFe}(\text{CO})_3\text{P}^-$  (P =  $\text{PPh}_3$ ,  $\text{PET}_3$ ,  $\text{PMe}_3$ ,  $\text{P}(\text{OMe})_3$ , and  $\text{P}(\text{OEt})_3$ ),  $^9,^{10}$   $\text{W}(\text{CO})_5\text{PPh}_3$ ,<sup>11</sup> and  $\text{W}(\text{CO})_5\text{P}(\text{OMe})_3$ <sup>12</sup> were prepared according to published procedures. Nitrogen was predried over molecular sieves prior to use. All other reagents were purchased from standard vendors as reagent or better grade and used without further purification.

**Preparation of  $\text{M}(\text{CO})_4\text{L}\cdot\text{THF}$ , M = Cr, W; L = CO. M = W; L =  $\text{P}(\text{OMe})_3$ ,  $\text{PPh}_3$ .** The general procedure was to load a 150-mL water-jacketed photovessel, flushed with  $\text{N}_2$ , with 1.00 g of  $\text{M}(\text{CO})_4\text{L}$  complex. A 90-mL portion of THF was added via cannula under  $\text{N}_2$ . The solution was photolyzed (450-W Hg vapor lamp) for 1 h, or until >90% conversion to  $\text{M}(\text{CO})_4\text{L}\cdot\text{THF}$  was attained, based on infrared: IR  $\nu(\text{CO})$  ( $\text{Cr}(\text{CO})_5\cdot\text{THF}$ ) 2074 w, 1938 s, 1894 m; ( $\text{W}(\text{CO})_5\cdot\text{THF}$ ) 2075 w, 1936 s, 1895 m; (*cis*- $\text{W}(\text{CO})_4\text{P}(\text{OMe})_3\cdot\text{THF}$ ) 2018 m, 1892 s (a composite of two bands), 1845 m; (*cis*- $\text{W}(\text{CO})_4\text{PPh}_3\cdot\text{THF}$ ) 2012 m, 1895 s (composite), 1847  $\text{m cm}^{-1}$ . A slow, steady stream of  $\text{N}_2$  bubbling through the solution during photolysis assists in removal of CO. These reagents were used in situ immediately after their generation.

**Preparation of  $[\text{PPN}][\text{HFeM}(\text{CO})_5]$ , M = W (1), Cr (3).** Details of the synthesis of 3 are appropriate to both. To an  $\text{N}_2$ -filled 100-mL Schlenk flask was added 1.00 g (1.41 mmol) of  $[\text{PPN}][\text{HFe}(\text{CO})_4]$ . Ninety milliliters of a  $1.57 \times 10^{-2}$  M solution (1.41 mmol) of  $\text{Cr}(\text{CO})_5\cdot\text{THF}$  as synthesized above was added via cannula to the flask which contained the iron hydride. The mixture was stirred for 5 min after which the solution was concentrated to 10 mL under vacuum. Hexane was slowly added to precipitate out an orange solid. The mother liquid was removed, and the solid was dissolved in diethyl ether and filtered through Celite. The orange solution was again concentrated to 10 mL, and hexane was slowly added while agitating to produce an orange powder. The mother liquid was removed via cannula and the solid washed twice with hexane. The dried orange solid weighed 1.17 g, a 92%

yield. Anal. (Galbraith Laboratories, Knoxville, TN) Anal. Calcd (Found) for 3,  $\text{C}_{45}\text{H}_{31}\text{NO}_9\text{PFeCr}$ : C, 60.02 (60.03); H, 3.47 (3.49); N, 1.56 (1.50). Anal. Calcd (Found) for 1,  $\text{C}_{45}\text{H}_{31}\text{NO}_9\text{PFeW}$ : C, 52.40 (52.26); H, 3.03 (3.06); N, 1.36 (1.44). IR and  $^1\text{H}$  NMR spectral characteristics are found in Table I;  $^{13}\text{C}$  NMR values are in Table II.

**Preparation of  $[\text{PPN}][\text{HFe}(\text{CO})_3(\text{P}(\text{OMe})_3)\text{W}(\text{CO})_5]$  (2).** A 90-mL,  $3.78 \times 10^{-3}$  M (0.34 mmol) portion of  $\text{W}(\text{CO})_5\cdot\text{THF}$  as synthesized above was transferred via cannula into a 100-mL Schlenk flask containing 275 mg (0.34 mmol) of  $[\text{PPN}][\text{trans-HFe}(\text{CO})_3\text{P}(\text{OMe})_3]$ . The solution was stirred for 5 min and then concentrated to 10 mL. Hexane was added to precipitate out a brown-yellow solid. After the mother liquid was removed, the solid was dried under vacuum. The solid was then redissolved in a 50:50 mixture of diethyl ether and THF and filtered through Celite, yielding a bright-orange solution. The solution was concentrated to 10 mL, and hexane was slowly added while agitating, forming a yellow solid which was washed twice with hexane and dried in vacuo. The yellow solid was recrystallized from diethyl ether/THF and hexane to yield 290 mg (0.26 mmol), a 76% yield, of 2. Anal. (Galbraith) Calcd (Found) for  $\text{C}_{47}\text{H}_{40}\text{P}_3\text{NO}_{11}\text{FeW}$ : C, 50.07 (50.06); H, 3.73 (3.58).

The  $[\text{PPN}][\text{HFe}(\text{CO})_3\text{P}(\text{OMe})_3]$ , M = W, P =  $\text{P}(\text{OEt})_3$ , 6,  $\text{PMe}_3$ , 7,  $\text{PET}_3$ , 8, and M = Cr, P =  $\text{PPh}_3$ , 9,  $\text{P}(\text{OMe})_3$ , 10, analogues to 2 were synthesized in the same method described above with similarly high yields of product. Spectral characteristics are listed in Table I.

**Preparation of  $[\text{PPN}][\text{HFe}(\text{CO})_4\text{W}(\text{CO})_4\text{P}]$ , P =  $\text{P}(\text{OMe})_3$  (11),  $\text{PPh}_3$  (12).** Into a 100-mL Schlenk flask was loaded 1.61 g (2.27 mmol) of  $[\text{PPN}][\text{HFe}(\text{CO})_4]$  and 70 mL of 0.032 M (2.27 mmol) *cis*- $\text{W}(\text{CO})_4\text{P}(\text{OMe})_3\cdot\text{THF}$ , freshly prepared as described above. The solution was stirred for 30 min and the solvent concentrated to 10 mL under vacuum. Hexane was slowly added until a precipitate formed. The hexane-THF supernatant was removed via cannula and the solid washed twice with hexane. After the solid was dried in vacuo, it was recrystallized from a mixture of (THF-diethyl ether)/hexane. The yellow-orange solid weighed 1.07 g (0.95 mmol) or 42% yield.

The  $\text{PPh}_3$  analogue of 10 was prepared in the exact same manner as described above. Spectral characteristics of both compounds are listed in Table I.

Elemental analysis of these compounds was not possible due to pronounced and rapid decomposition even in the solid state.

**Preparation of  $[\text{Et}_4\text{N}][\text{FeCr}(\text{CO})_9]$  (13).** Into a 100-mL Schlenk flask was loaded 1.00 g (2.03 mmol) of  $[\text{Et}_4\text{N}][\text{HFeCr}(\text{CO})_9]$  which was prepared in the same manner as 3 using  $[\text{Et}_4\text{N}][\text{HFe}(\text{CO})_4]$  instead of  $[\text{PPN}][\text{HFe}(\text{CO})_4]$ . A 20-mL portion of THF was added via syringe to the flask. To the orange solution was added 0.33 g (2.03 mmol) of  $\text{Et}_4\text{NOH}$  (in the form of 25% w/w  $\text{Et}_4\text{NOH}/\text{MeOH}$  solution). The solution was allowed to stir until an orange precipitate was formed. The mother liquid was removed, and the solid was washed twice with THF and then was dried in vacuo. The solid was dissolved in  $\text{CH}_3\text{CN}$  and filtered through Celite. Addition of diethyl ether precipitated 13 as an

(8) Darensbourg, M. Y.; Darensbourg, D. J.; Barros, H. L. C. *Inorg. Chem.* **1978**, *17*, 297.

(9) Chen, Y. S.; Ellis, J. E. *J. Am. Chem. Soc.* **1982**, *104*, 1141.

(10) Ash, C. E.; Delord, T.; Simmons, D.; Darensbourg, M. Y. *Organometallics* **1986**, *5*, 17.

(11) Connor, J. E.; Jones, E. M.; McEwen, G. K. *J. Organomet. Chem.* **1972**, *43*, 357.

(12) Mathieu, R.; Lenzi, M.; Poilblanc, R. *Inorg. Chem.* **1970**, *9*, 2030.

Table III. Summary of Crystallographic Data

formula	[PPN] <sub>2</sub> [FeCr(CO) <sub>9</sub> ], <b>4</b>	[PPN][HFeCr(CO) <sub>9</sub> ], <b>3</b>	[PPN][HFeW(CO) <sub>9</sub> ], <b>1</b>	[PPN][[(CO) <sub>3</sub> P(OMe) <sub>3</sub> FeHW(CO) <sub>5</sub> ], <b>2</b>
<i>M<sub>w</sub></i>	1478.2	899.53	1031.4	1127.5
space group	<i>P</i> $\bar{1}$	<i>P</i> $\bar{1}$	<i>P</i> $\bar{1}$	<i>P</i> 2 <sub>1</sub> / <i>N</i>
cell parameters				
<i>a</i> , Å	13.882 (2)	11.717 (2)	14.099 (5)	12.200 (2)
<i>b</i> , Å	22.825 (4)	14.095 (3)	11.601 (5)	12.461 (2)
<i>c</i> , Å	13.067 (2)	14.283 (2)	14.148 (5)	32.032 (4)
$\alpha$ , deg	96.07 (1)	92.18 (2)	95.53 (3)	90.00
$\beta$ , deg	117.57 (1)	117.51 (1)	118.23 (3)	96.40 (1)
$\gamma$ , deg	87.27 (1)	95.78 (2)	92.39 (3)	90.00
cell vol, Å <sup>3</sup>	3650 (2)	2072 (1)	2026 (3)	4838 (2)
<i>Z</i>	2	2	2	4
crystal dimens., mm	0.28 × 0.33 × 0.42	0.30 × 0.32 × 0.35	0.32 × 0.28 × 0.36	0.30 × 0.25 × 0.30
$\rho_{\text{calcd}}$ , g cm <sup>-3</sup>	1.342	1.44	1.69	1.65
$\mu$ , cm <sup>-1</sup>	5.1	7.36	33.89	29.8
radiation, Å	Mo K $\alpha$ ( $\lambda = 0.71069$ )	Mo K $\alpha$ ( $\lambda = 0.71069$ )	Mo K $\alpha$ ( $\lambda = 0.71069$ )	Mo K $\alpha$ ( $\lambda = 0.71069$ )
std. reflections	0-43,6-1-4,3-5-1	0-14,200,50-1	12-1,-131,022	00-4,-1-24,1-13
2 $\theta$ range, deg	0-40	3-45	3-45	3-48
no. of reflections used in refinement				
( $F_o^2 > 3\sigma(F_o^2)$ )	3905	1321	3637	1769
no. of parameters	505	247	348	336
$R^a$	0.050	0.066	0.053	0.080
$R_w^b$	0.060	0.053	0.061	0.069
residual electron density, e <sup>-</sup> /Å <sup>3</sup>	0.41	0.39	0.36	0.74
refinement method	SDP	SHELXTL <sup>15</sup>	SDP	SDP
diffractometer	<i>c</i>	<i>d</i>	<i>c</i>	<i>d</i>

<sup>a</sup> $R = \sum ||F_o| - |F_c|| / \sum |F_o|$ . <sup>b</sup> $R_w = [\sum w(|F_o| - |F_c|)^2 / \sum w(F_o)^2]^{1/2}$ . <sup>c</sup>Enraf-Nonius CAD-4. <sup>d</sup>Nicolet P3F.

orange crystalline solid which produced 1.25 g, or a 95% yield.

**Preparation of [Et<sub>4</sub>N]<sub>2</sub>[FeW(CO)<sub>9</sub>] (14).** The preparation of **14** followed in the same method as **13** with a similarly high yield.

**Preparation of [PPN]<sub>2</sub>[FeCr(CO)<sub>9</sub>] (4) and [PPN]<sub>2</sub>[FeW(CO)<sub>9</sub>] (15).** To a 100-mL Schlenk flask was loaded 0.64 g (1.11 mmol) of PPNC1 and 1.00 g (1.11 mmol) of **3**. The flask was evacuated and back-filled with nitrogen. A 25-mL portion of THF was added via cannula into the flask. Butyllithium was then slowly added dropwise via syringe until a dark-red solution was obtained and no gas bubbles evolved upon further addition of BuLi. The solution was allowed to stand for 30 min during which time a red precipitate formed. The mother liquid was removed and the solid washed twice with THF. The red solid was dissolved in 10 mL of CH<sub>3</sub>CN and filtered through Celite. The solution was concentrated to 10 mL, and diethyl ether was slowly added while agitating to precipitate an orange-red solid. The solid was washed twice with hexane and dried in vacuo. Anal. (Galbraith) Calcd (Found) for C<sub>81</sub>H<sub>60</sub>P<sub>4</sub>N<sub>2</sub>O<sub>9</sub>FeCr: C, 67.70 (67.36); H, 4.21 (4.44).

**X-ray Structural Analysis of 1.** A clear, yellow-orange crystal of **1** of approximate size 0.32 mm × 0.28 mm × 0.36 mm was mounted in epoxy inside a glass capillary tube for atmospheric protection. All data were collected on an Enraf-Nonius CAD-4 computer-automated diffractometer at -103 °C using Mo K $\alpha$  radiation. Precise lattice parameters were determined from 25 well-centered reflections (6° <  $\theta$  < 28°) to give the triclinic cell parameters found in Table III.

The intensities of 5671 reflections were measured by using the  $\theta$ -2 $\theta$  scan method. Data were collected in the range of 1.5° <  $\theta$  < 22.5° for reflections with indices  $h, k \geq 0, \pm l$ . The intensity data were corrected for Lorentz and polarization effects. An empirical absorption correction ( $\mu(\text{Mo K}\alpha) = 33.89 \text{ cm}^{-1}$ ) was made based on aximuthal scans of eight reflections near  $\chi = 90^\circ$ . Periodically measured intensity standard reflections demonstrated no significant variation in intensity during collection. Details of intensity data collections are listed in Table III.

The positions of the W and Fe atoms were determined by applications of the direct methods programs of the SDP crystallographic computer package. The remaining non-hydrogen atoms were located from subsequent difference Fourier maps. All hydrogens on the cation were included in idealized, calculated positions with fixed thermal parameters. The structure was refined by weighted ( $w = 1/\sigma^2(F_o)$ ), full-matrix least-squares refinement, minimizing the function  $(w|F_o| - |F_c|)^2$ . Neutral atomic scattering factors<sup>13</sup> were applied to all atoms. All atoms of the anion were allowed to refine anisotropically except C7, while the remaining non-hydrogen atoms were refined isotropically. Refinement converged at  $R = 0.053$  ( $R_w = 0.061$ ) for 3637 reflections ( $F^2 > 3\sigma(F^2)$ ) and 348 variables. The final cycle of least squares had a maximum

shift/esd of less than 0.01. A final difference Fourier map had maximum peak of residual electron density of 0.36e<sup>-</sup>/Å<sup>3</sup>, of no apparent chemical significance.

**X-ray Structural Analysis of 2.** A clear, yellow, irregularly shaped crystal was used for X-ray intensity data collection. Precise lattice parameters were determined by 25 well-centered reflections (10° <  $\theta$  < 15°) to give the monoclinic cell parameters given in Table III.

The intensities of 7925 reflections were measured at 21 °C by using the  $\omega$  scan method. Data were collected in the range 1.5° <  $\theta$  < 24° for reflections with indices  $h, k \geq 0, \pm l$ . The three intensity standards showed 30.6% loss in intensity during the 170.8 h of X-ray exposure. A decay correction was applied. In addition, a semiempirical absorption correction was made ( $\mu = 29.8 \text{ cm}^{-1}$ ) based on aximuthal scans of nine reflections with an Eulerian angle  $\chi$  near 90°.

The structure was solved and refined in a manner similar to **1**. Anomalous dispersion corrections<sup>14</sup> were applied to all atoms. All atoms of the anion except O6, O8, and C2-C13 were allowed to refine anisotropically, while the remaining non-hydrogen atoms of the structure were refined isotropically. Positional parameter of C8 was fixed in the *y* coordinate to 0.110, while the remaining variables were allowed to vary. Refinement values are in Table III.

**X-ray Structural Analysis of 3.** A clear, red, irregularly shaped crystal of **3** was used for data collection. The intensity of 5744 reflections were measured at 21 °C by using the  $\omega$  scan technique. Data were collected in the range 1.5° <  $\theta$  < 22.5° for reflections with indices  $h \geq 0, \pm k, \pm l$ . The intensity data were corrected for Lorentz and polarization effects to yield observed structure factors. No correction was made for absorption effects ( $\mu = 7.36 \text{ cm}^{-1}$ ). Intensity standard reflections periodically measured during data collection demonstrated no significant variation during the course of the experiment. Details of intensity data measurement and refinement are listed in Table III.

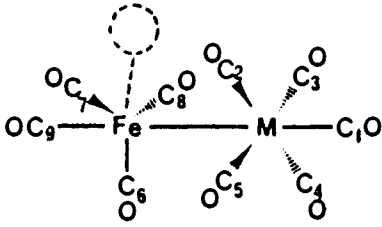
After numerous attempts to solve the structure by direct methods (SOLV), the positions of the Cr and Fe atoms were determined by the automatic Patterson solution option of the SHELXTL<sup>15</sup> crystallographic computing system. The remaining non-hydrogen atoms of the structure were located by subsequent least squares and difference Fourier synthesis. The structure was refined by weighted ( $w = 1/\sigma^2(F) + 0.00021(F^2)$ ), full-matrix least squares, minimizing the function  $(w|F_o| - |F_c|)^2$ . All atoms of the anion as well as the N and the two P atoms of the cation were refined anisotropically. The phenyl rings of the cation were refined as rigid bodies with idealized, hexagonal geometry. The temperature factors of the phenyl carbon atoms were tied together and refined as a

(14) Cromer, D. T.; Waber, J. T. In *International Tables for X-ray Crystallography*; The Kynock: Birmingham, England, 1974; Vol. IV, Table 2.3.1.

(15) Sheldrick, G. M. In *Nicolet SHELXTL Operations Manual*; Nicolet XRD: Cupertino, CA, 1979.

(13) Cromer, D. T.; Waber, J. T. In *International Tables for X-ray Crystallography*; The Kynock: Birmingham, England, 1974; Vol. IV, Table 2.2B.



Table IV.<sup>a</sup> Bond Distances (Å) and Bond Angles (deg)


	FeCr(CO) <sub>9</sub> <sup>2-</sup>	HFeCr(CO) <sub>9</sub> <sup>-</sup>	HFeW(CO) <sub>9</sub> <sup>-</sup>	HFeW(CO) <sub>8</sub> P(OMe) <sub>3</sub> <sup>-</sup>	PPh <sub>3</sub> AuFeW(CO) <sub>9</sub> <sup>-</sup>
	Distances				
M-Fe	2.941 (2)	2.956 (7)	2.997 (2)	2.974 (5)	3.012 (3)
M-C1	1.804 (9)	1.808 (26)	1.896 (12)	1.97 (4)	1.880 (25)
M-C2	1.850 (9)	1.889 (29)	2.013 (13)	2.12 (4)	2.028 (28)
M-C3	1.857 (9)	1.907 (19)	2.023 (13)	1.97 (5)	1.820 (29)
M-C4	1.895 (9)	1.908 (25)	2.022 (13)	1.93 (4)	2.048 (26)
M-C5	1.874 (9)	1.898 (20)	2.038 (12)	2.06 (4)	1.872 (29)
Fe-C6	1.757 (8)	1.805 (26)	1.774 (12)	1.82 (4)	1.780 (30)
Fe-C7	1.756 (9)	1.745 (25)	1.798 (13)	1.79 (5)	1.756 (28)
Fe-C8	1.729 (9)	1.748 (22)	1.739 (13)	1.708 (11)	1.823 (23)
Fe-C9	1.718 (9)	1.752 (19)	1.741 (11)	2.143 (11) <sup>b</sup>	1.782 (26)
Fe-Au					2.520 (3)
Au-P					2.268 (5)
	Angles				
C1-M-C2	95.1 (3)	90.5 (13)	90.3 (5)	92 (1)	86.7 (11)
C1-M-C3	90.1 (3)	89.1 (10)	89.5 (4)	89 (2)	88.3 (12)
C1-M-C4	96.5 (4)	91.1 (12)	88.9 (5)	91 (2)	92.6 (11)
C1-M-C5	89.3 (3)	89.8 (10)	89.9 (4)	93 (1)	89.3 (12)
C2-M-C3	94.1 (4)	89.7 (11)	90.2 (5)	89 (2)	91.2 (12)
C2-M-C4	167.8 (4)	178.4 (10)	178.4 (5)	178 (2)	179.0 (6)
C2-M-C5	88.5 (3)	91.2 (11)	87.9 (4)	92 (1)	87.4 (12)
C3-M-C4	89.8 (4)	90.4 (10)	91.0 (5)	92 (3)	89.5 (12)
C3-M-C5	177.3 (4)	178.5 (11)	178.1 (5)	178 (2)	177.3 (13)
C4-M-C5	87.7 (4)	88.7 (11)	90.9 (4)	89 (2)	91.9 (12)
C6-Fe-C7	117.5 (4)	100.7 (11)	98.5 (5)	98 (2)	102.0 (7)
C6-Fe-C8	125.1 (4)	101.2 (12)	101.9 (5)	101 (2)	101.7 (6)
C6-Fe-C9	94.6 (4)	99.8 (10)	99.4 (5)	98 (1) <sup>c</sup>	100.1 (2)
C7-Fe-C8	112.9 (4)	147.8 (12)	147.2 (5)	153 (2)	144.1 (12)
C7-Fe-C9	99.6 (4)	100.4 (10)	101.1 (5)	98 (1) <sup>d</sup>	99.5 (8)
C8-Fe-C9	97.3 (4)	98.8 (10)	100.6 (5)	98 (2) <sup>e</sup>	102.5 (6)
Fe-C9-O9	179.6 (8)	177.3 (18)	179 (1)		178.1 (10)
Fe-C6-O6	175.8 (7)	176.4 (21)	174.3 (9)	176 (3)	176.8 (10)
Fe-C7-O7	174.8 (7)	171.7 (19)	171 (1)	176 (4)	171.6 (26)
Fe-C8-O8	174.2 (8)	171.4 (22)	174 (1)	176 (4)	171.7 (9)
Au-Fe-W					82.7 (1)
Fe-Au-P					174.4 (2)
Au-Fe-C7					78.7 (8)
Au-Fe-C8					74.7 (6)

<sup>a</sup>The uniform numbering scheme given in the above table has been changed from the ORTEPS in the text. The conversion from C atoms 1,2,3,4,5,6,7,8,9 in scheme to C atoms in ORTEPS are FeCr(CO)<sub>9</sub><sup>2-</sup> 9,8,7,6,5,2,3,1,4; HFeCr(CO)<sub>9</sub><sup>-</sup> 1,2,3,4,5,7,6,8,9; HFeW(CO)<sub>9</sub><sup>-</sup> 3,2,4,1,5,8,6,7,9; HFeW(CO)<sub>8</sub>P(OMe)<sub>3</sub><sup>-</sup> 1,5,4,2,3,7,8,6; Ph<sub>3</sub>AuFeW(CO)<sub>9</sub><sup>-</sup> 1,2,3,4,5,6,7,8,9 (i.e., the same). <sup>b</sup>P-Fe bond distance. <sup>c</sup>P-Fe-C6 bond angle. <sup>d</sup>P-Fe-C7 bond angle. <sup>e</sup>P-Fe-C8 bond angle.

has been characterized by crystallography in numerous cases and typically found to have a P-N-P angle of ~141°. The same was observed in the structures determined in this work. Table III is a summary of the crystallographic data, and Table IV lists selected bond distances and bond angles for all anions. In order to facilitate discussion, these are referenced to a common numbering scheme for all CO groups. Complete listings of all bond distances and angles for the heterobimetallic anions and corresponding cations are deposited as supplementary material.

In all anions, the group 6 metal is in a regular octahedral coordination sphere. All CO ligands are terminal, and the M-CO show little deviation from linearity except in the following cases: The equatorial Fe-C-O groups on HFeCr(CO)<sub>9</sub><sup>-</sup> (3), HFeW(CO)<sub>9</sub><sup>-</sup> (1), and Ph<sub>3</sub>AuFeW(CO)<sub>9</sub><sup>-</sup> (5) have angles of 172°. Inspection of molecular models indicates a random angularity, and only one such group might represent an underdeveloped semibridging CO ligand. That is, the Fe-C-O bend inclines carbon toward Cr or W for only one equatorial Fe-CO. A cautious interpretation would place no significance on these deviations from linearity. In view, however, of the ease of intrametallic CO mobility in anions 1, 3, and 5, *vide infra*, the case

for incipient semibridging CO's gains credibility.

There is a significant trans influence of the Fe(CO)<sub>4</sub> metal-loanion ligand on the group 6 metal-C<sub>ax</sub> bond in anions 1, 3, and 4. For example, in dianion 3, the Cr-C<sub>1</sub> or Cr-C<sub>ax</sub> bond distance is 0.1 Å shorter than the average Cr-C<sub>eq</sub> distance. On protonation, leading to anion 3, there are no significant differences in Cr-C distances, and the trans influence of 0.1 Å persists. A similar difference in W-C<sub>ax</sub> vs. W-C<sub>eq</sub> in 1 is observed. The poorer quality of structures 2 and 5 will not permit interpretation of possible W-C distance differences.

The coordination geometry of Fe in FeCr(CO)<sub>9</sub><sup>2-</sup> may be described as a pseudotrigonal bipyramid or a perturbed tetrahedron, Figure 1. The Fe(CO)<sub>4</sub> fragment in FeCr(CO)<sub>9</sub><sup>2-</sup> is, within experimental error, *practically identical* with that of HFe(CO)<sub>4</sub><sup>-</sup>.<sup>17</sup> The Fe-C<sub>eq</sub> bond distances average to 1.75 Å in both cases, the Fe-C<sub>ax</sub> distance is 1.72 Å in both, and the average C<sub>ax</sub>-Fe-C<sub>eq</sub> angle is 99.1° in HFe(CO)<sub>4</sub><sup>-</sup> and 97.3° in (OC)<sub>5</sub>CrFe(CO)<sub>4</sub><sup>2-</sup>. Both structures may be interpreted as tetrahedral Fe(CO)<sub>4</sub><sup>2-</sup> perturbed by an electrophile interacting through one tetrahedral

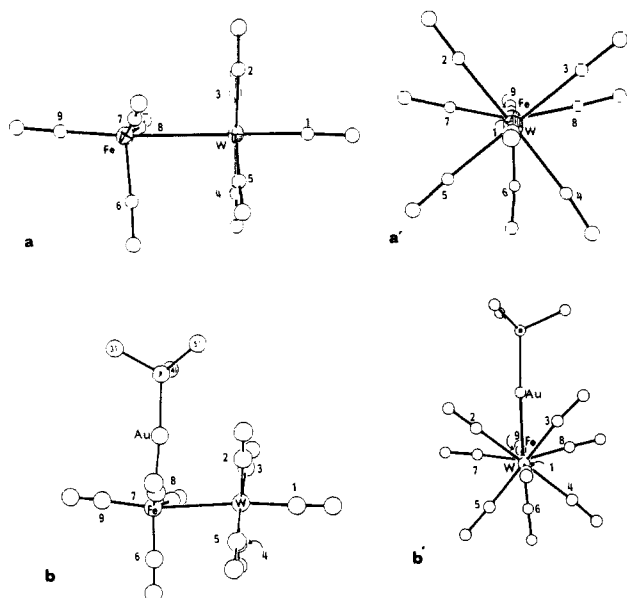
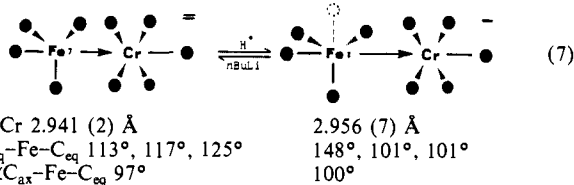


**Figure 4.** Comparison of the molecular structures of  $\text{HFeW}(\text{CO})_9^-$  and  $\text{Ph}_3\text{PAuFeW}(\text{CO})_9^-$ : (a and b) side views and (a' and b') along the  $(\text{O1C1})-\text{W}-\text{Fe}-(\text{C909})$  vectors. Only the  $\alpha$  carbons on the phenyl rings in b and b' are shown for clarity.

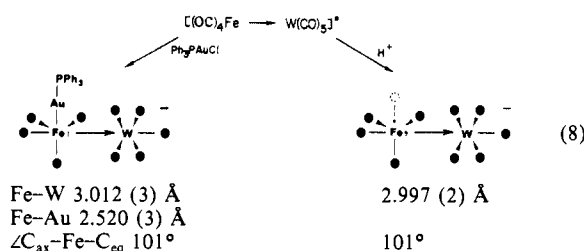
face. The surprising feature of this analysis is that the stereochemical requirements of the very different electrophiles involved,  $\text{H}^+$  vs.  $\text{M}(\text{CO})_5^0$ , appear to be of little consequence to  $\text{Fe}(\text{CO})_4^{2-}$ .

The stick drawings of eq 7 emphasize the scant structural changes associated with protonation of  $\text{FeCr}(\text{CO})_9^{2-}$ . The metal-metal bond lengthens by only 0.01 Å, and the only angle change of note is an opening of one  $\text{C}_{\text{eq}}-\text{Fe}-\text{C}_{\text{eq}}$  angle from an average of  $118-148^\circ$ . The hydride ligand, not located in all these structure



analyses, is thus presumed to be located solely on the Fe in  $\text{HFeCr}(\text{CO})_9^-$ . This presumption is supported by recent theoretical calculations<sup>5</sup> and by analogy to  $\text{HRe}_2(\text{CO})_9^-$ , reported to be of cis geometry on basis of its C-13 spectrum.<sup>18</sup>

Further evidence for the terminal character of the hydride ligand in these mixed metal hydrides was obtained in comparison of the structures of  $\text{HFeW}(\text{CO})_9^-$  and  $\text{Ph}_3\text{PAuFeW}(\text{CO})_9^-$ ,<sup>6</sup> Figure 4a and 4b, and the stick drawings of eq 8. The  $\text{Ph}_3\text{PAu}$  ligand rests



solely on Fe, opening the  $\text{C}_7-\text{Fe}-\text{C}_3$  angle from trigonal in the parent dianion to  $144^\circ$ . The analogous angle in  $\text{HFeW}(\text{CO})_9^-$  is  $147^\circ$ . Thus the open site in the  $\text{HFeW}(\text{CO})_9^-$  structure, Figure 4a and 4a', corresponds exactly to the position of  $\text{Ph}_3\text{PAu}$  in Figure 4b and 4b'. The structural assignment of the hydride ligand in  $\text{HFeM}(\text{CO})_9^-$  is established as that of a terminal ligand. This conclusion is reasonable in terms of a structure composition having

**Table V.** Atomic Positional and Equivalent Isotropic Thermal Parameters for **1<sup>a</sup>**

atom	X	Y	Z	$B_{\text{eq}}$ , Å <sup>2</sup>
W	0.34552 (5)	0.00578 (6)	0.78895 (5)	1.70 (1)
Fe	0.1468 (2)	0.1321 (2)	0.7056 (2)	1.96 (5)
P1	0.7075 (3)	-0.2825 (4)	0.8295 (3)	1.56 (9)
P2	0.7489 (3)	-0.3747 (4)	0.7312 (3)	1.66 (9)
O1	0.1995 (9)	-0.225 (1)	0.6443 (9)	3.8 (3)
O2	0.5005 (8)	0.2289 (9)	0.9433 (9)	3.0 (3)
O3	0.5452 (9)	-0.1347 (9)	0.8712 (9)	3.4 (3)
O4	0.3834 (9)	0.070 (1)	0.5956 (9)	4.3 (3)
O5	0.3020 (8)	-0.076 (1)	0.9750 (9)	3.3 (3)
O6	0.2748 (9)	0.278 (1)	0.9148 (9)	3.8 (3)
O7	0.1292 (9)	0.021 (1)	0.5006 (9)	3.7 (3)
O8	0.0472 (9)	-0.060 (1)	0.7598 (9)	3.2 (3)
O9	-0.0367 (9)	0.269 (1)	0.6167 (9)	3.5 (3)
N	0.7413 (9)	-0.141 (1)	0.7688 (9)	2.0 (3)
C1	0.251 (1)	-0.141 (1)	0.6940 (9)	2.4 (4)
C2	0.4434 (9)	0.1509 (9)	0.8869 (9)	2.4 (4)
C3	0.4683 (9)	-0.0778 (9)	0.8401 (9)	1.6 (3)
C4	0.368 (1)	0.043 (1)	0.664 (1)	3.8 (5)
C5	0.320 (1)	-0.039 (2)	0.914 (1)	2.3 (4)
C6	0.2296 (8)	0.2165 (9)	0.839 (1)	2.5 (4)
C7	0.141 (1)	0.065 (1)	0.587 (1)	2.3 (3)
C8	0.091 (1)	0.016 (1)	0.746 (1)	2.4 (4)
C9	0.038 (1)	0.215 (1)	0.654 (1)	2.3 (4)
C10	0.7186 (9)	0.272 (1)	0.7824 (9)	1.7 (3)*
C11	0.783 (1)	0.254 (1)	0.732 (1)	2.1 (3)*
C12	0.796 (1)	0.142 (1)	0.699 (1)	2.4 (3)*
C13	0.742 (1)	0.043 (1)	0.714 (1)	3.0 (3)*
C14	0.678 (1)	0.060 (1)	0.764 (1)	2.9 (3)*
C15	0.6673 (9)	0.175 (1)	0.7994 (9)	1.9 (3)*
C20	0.5714 (1)	0.424 (1)	0.8078 (9)	1.6 (3)*
C21	0.551 (1)	0.495 (1)	0.880 (1)	2.4 (3)*
C22	0.443 (1)	0.510 (1)	0.854 (1)	2.7 (3)*
C23	0.361 (1)	0.449 (1)	0.763 (1)	2.7 (3)*
C24	0.380 (1)	0.379 (1)	0.690 (1)	2.5 (3)*
C25	0.4865 (9)	0.364 (1)	0.7122 (9)	1.8 (3)*
C30	0.7902 (9)	0.443 (1)	0.9727 (9)	1.8 (3)*
C31	0.768 (1)	0.372 (1)	1.039 (1)	2.6 (3)*
C32	0.830 (1)	0.393 (1)	1.152 (1)	2.6 (3)*
C33	0.915 (1)	0.483 (1)	1.200 (1)	2.8 (3)*
C34	0.938 (1)	0.550 (1)	1.136 (1)	2.6 (3)*
C35	0.878 (1)	0.530 (1)	1.022 (1)	2.6 (3)*
C40	0.6205 (9)	0.682 (1)	0.6581 (9)	1.5 (2)*
C41	0.606 (1)	0.755 (1)	0.581 (1)	2.4 (3)*
C42	0.508 (1)	0.806 (1)	0.531 (1)	3.2 (3)*
C43	0.423 (1)	0.781 (1)	0.554 (1)	2.7 (3)*
C44	0.441 (1)	0.708 (1)	0.634 (1)	3.4 (3)*
C45	0.540 (1)	0.659 (1)	0.685 (1)	2.7 (3)*
C50	0.8364 (9)	0.733 (1)	0.8455 (9)	1.6 (2)*
C51	0.789 (1)	0.806 (1)	0.892 (1)	2.2 (3)*
C52	0.856 (1)	0.880 (1)	0.985 (1)	3.1 (3)*
C53	0.968 (1)	0.879 (1)	1.034 (1)	2.5 (3)*
C54	1.015 (1)	0.808 (1)	0.985 (1)	2.1 (3)*
C55	0.948 (1)	0.734 (1)	0.890 (1)	2.2 (3)*
C60	0.8072 (9)	0.609 (1)	0.6412 (9)	1.6 (2)*
C61	0.789 (1)	0.503 (1)	0.578 (1)	2.2 (3)*
C62	0.834 (1)	0.491 (1)	0.509 (1)	2.6 (3)*
C63	0.899 (1)	0.588 (1)	0.506 (1)	2.7 (3)*
C64	0.916 (1)	0.692 (1)	0.568 (1)	2.3 (3)*
C65	0.869 (1)	0.705 (1)	0.636 (1)	1.8 (3)*

<sup>a</sup>Starred atoms were refined isotropically. Equivalent isotropic  $B$  defined as one-third of the trace of the orthogonalized  $B_{ij}$  tensor for all unstarred atoms.

as its basis  $\text{Fe}(\text{CO})_4^{2-}$  interacting with two nucleophiles:  $\text{H}^+$  and  $\text{M}(\text{CO})_5^0$  or, in the isolobal analogy,<sup>19</sup>  $\text{Ph}_3\text{PAu}^+$  and  $\text{M}(\text{CO})_5^0$ . The coordinative saturation of  $\text{M}(\text{CO})_5^0$  prevents H-M or Au-M bond formation.

The structure of  $\text{HFeM}(\text{CO})_9^-$  deviates radically from the homobimetallic parents:  $(\mu\text{-H})(\mu\text{-CO})_2\text{Fe}(\text{CO})_6^-$  and  $(\mu\text{-H})\text{M}_2(\text{CO})_{10}^-$  ( $\text{M} = \text{Cr}, \text{Mo}, \text{and W}$ ).<sup>20</sup> The former has a

(19) (a) Hoffmann, R. *Angew. Chem., Int. Ed. Engl.* 1982, 21, 711. (b) Halpern, J. *Adv. Chem. Ser.* 1968, 70, 1. (c) Mingos, M. P.; Evans, D. G. *J. Organomet. Chem.* 1982, 232, 171. (d) Stone, F. G. A. *Angew. Chem., Int. Ed. Engl.* 1984, 23, 89.

(18) Casey, C. P.; Neumann, S. M. *J. Am. Chem. Soc.* 1978, 100, 2544.







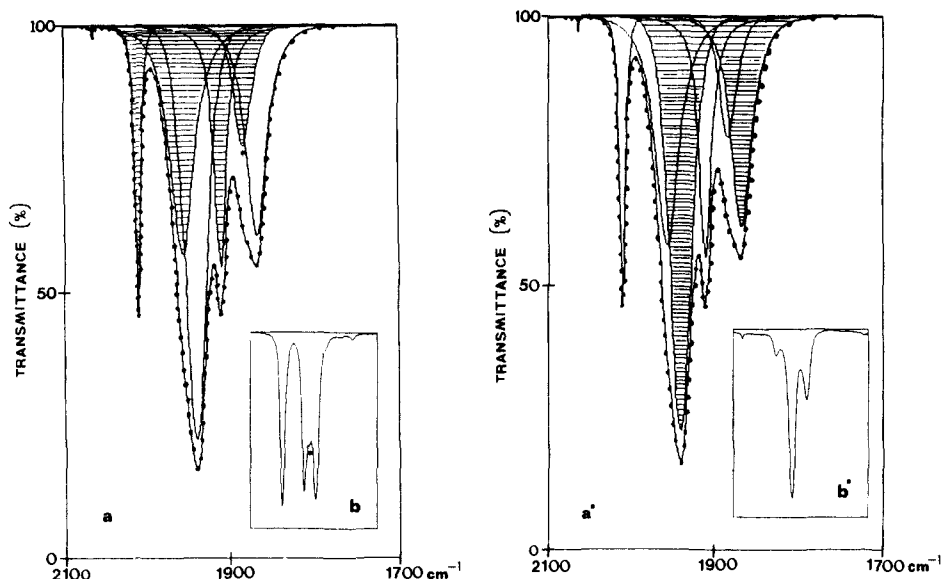
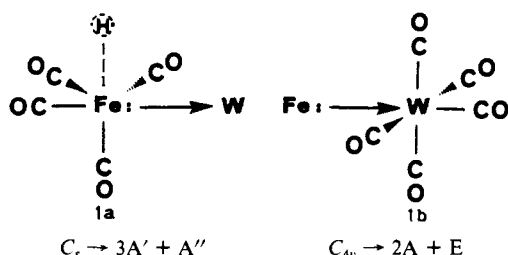


Figure 5.  $\nu(\text{CO})$  spectrum of  $\text{PPN}^+\text{HFeW}(\text{CO})_9^-$  (dotted line) deconvoluted into seven bands. The four hatch-marked bands in a were similar to the band pattern of  $(\text{Ph}_3\text{PAu})_2\text{Fe}(\text{CO})_4$ , reproduced in the inset b. Note that the medium band in between two stronger bands (starred in b) has moved to the right in the  $\text{HFeW}(\text{CO})_9^-$  spectrum (starred in a). The remaining three bands made evident in a' closely resemble the  $\nu(\text{CO})$  IR of  $\text{W}(\text{CO})_5\cdot\text{THF}$ , inset b'.

Fe-M stretches have not as yet been detected.

Although the CO stretching vibrations of the component metalloligand → metal acceptor complexes are expected to couple, we have analyzed the  $\nu(\text{CO})$  IR spectrum of **1** in terms of the fragments **1a** and **1b**. A maximum of seven bands is possible,



assuming the donor ligand **1a** is of pseudo- $C_s$  symmetry. In fact, the iron-carbonyl arrangement of **1a** suggests that substantial tetrahedral character remains associated with the iron, an arrangement similar to that of  $\text{H}_2\text{Fe}(\text{CO})_4$ ,<sup>26</sup>  $[\text{CdFe}(\text{CO})_4]_4$ ,<sup>27</sup> or  $(\text{Ph}_3\text{PAu})_2\text{Fe}(\text{CO})_4$ .<sup>28</sup> If a  $\nu(\text{CO})$  IR pattern similar to that of  $(\text{Ph}_3\text{PAu})_2\text{Fe}(\text{CO})_4$  is subtracted from the spectrum of  $\text{HFeW}(\text{CO})_9^-$ , a three-band pattern remains which very reasonably fits the expectations for  $C_{4v}$   $\text{L}:\text{W}(\text{CO})_5$ :  $A_1^2(w)$ ,  $E(s)$ ,  $1941$ , and  $A_1^1(m)$ ,  $1868$ ; in  $\text{W}(\text{CO})_5\cdot\text{THF}$ ,  $A_1^2(w)$   $2072$ ;  $E(s)$   $1927$  and  $A_1^1(m)$   $1882$   $\text{cm}^{-1}$ .<sup>29</sup> A complete  $\nu(\text{CO})$  analysis of **1**, under  $C_s$  symmetry, gives nine active IR bands. We cannot rule out the possibility of overlapping bands and coupled vibrations. The above interpretation may be overly simplistic. Nevertheless the chemistry of **1** and its congeners is supportive of localized negative charge on the more electronegative metal, or 18-electron donor ligand fragment.

The above analysis suggested the most intense band of the spectral envelope of the dimers to be due to a composite of both

metal centers. A similar analysis for the P-substituted dimers also suggests the most intense  $\nu(\text{CO})$  band to be due to both centers. Hence, the position of this major band is diagnostic of the electron density on the CO groups and, as displayed in Table I, agrees with the generally accepted order of ligand donor abilities.

The dianions  $\text{FeM}(\text{CO})_9^{2-}$  show fewer  $\nu(\text{CO})$  band maxima and very broad bands. Their spectra are counterion-dependent. For example, the presence of  $\text{Li}^+$  shifts the lower frequency bands by ca.  $30$   $\text{cm}^{-1}$  to higher values. This is consistent with  $\text{Li}^+$  counterion interaction at a metal, presumably Fe, center.<sup>30</sup>

The proton chemical shift values as well as P-H and W-H coupling constants of these mixed metal hydrides show no easily interpretable patterns (Table I). The hydride resonances of **1** and **2** are upfield of  $\text{HFe}(\text{CO})_4^-$  ( $\delta$   $-8.79$ )<sup>8</sup> and of  $\text{HFe}_2(\text{CO})_8^-$  ( $\delta$   $-8.45$ )<sup>31</sup> and are actually more similar to the  $\mu\text{-HM}_2(\text{CO})_{10}^-$  complexes ( $\delta$   $-12.6$  and  $-19.5$  for  $M = \text{W}$  and  $\text{Cr}$ , respectively).<sup>32</sup> Those mixed metal hydrides containing Cr show higher upfield shifts than those containing W. P-donor ligand ( $\text{PPh}_3$  excepted) substitution on the Fe center shifts the hydride resonance upfield by ca.  $1$  ppm for  $M = \text{W}$  and by  $2$  ppm for  $M = \text{Cr}$ , as compared to the all-CO anion. A small shift, opposite in direction, is observed for  $\text{PPh}_3$  and  $M = \text{Cr}$ ; no change is observed for  $\text{PPh}_3$  and  $M = \text{W}$ .

For all  $\text{HFe}(\text{CO})_3\text{PM}(\text{CO})_5^-$  anions, the P-H coupling is small, ca.  $20$ – $27$  Hz. Even so, these values are larger than  $J_{\text{P-H}}$  of the monomeric *trans*- $\text{HFe}(\text{CO})_3\text{P}$ .<sup>10</sup> Despite the *trans* arrangement of H and P in the latter, the  $J_{\text{P-H}}$  are on the order of  $4$ – $15$  Hz and are temperature-dependent.<sup>10</sup> The larger coupling here reflects the pseudooctahedral arrangement of ligands about Fe and, presumably, the greater involvement of the s orbital in the two-bond coupling. (The orbital coupling in *trans*- $\text{HFe}(\text{CO})_3\text{P}^-$  is mainly  $d_{z^2} p_z$  in character.) Interestingly, the  $J_{\text{P-H}}$  for  $\text{HFe}(\text{CO})_4\text{W}(\text{CO})_4\text{P}^-$ , assumed to be three-bond couplings,<sup>33</sup>  $\text{H-Fe-W-P}$ , are the same as the two-bond couplings,  $\text{P-Fe-H}$  in  $\text{HFe}(\text{CO})_3\text{PW}(\text{CO})_5^-$ . For comparison, the  $J_{\text{P-H}}$  values of the monomeric

(30) Darendbourg, M. Y. *Prog. Inorg. Chem.* **1985**, *33*, 221.

(31) Collman, J. P.; Finke, R. G.; Matlock, P. L.; Wahren, R.; Komoto, R. G.; Brauman, J. I. *J. Am. Chem. Soc.* **1978**, *100*, 1119.

(32) (a) Hayter, R. G. *J. Am. Chem. Soc.* **1966**, *88*, 4376. (b) Darendbourg, M. Y.; Deaton, J. C. *Inorg. Chem.* **1981**, *20*, 1644.

(33) The ab initio calculations of Halpin and Hall<sup>5</sup> yield contour maps of the  $\text{H-Fe-M}$  ( $M = \text{Mo}$  for the calculation) HOMOs which show the primary Fe-Mo bonding molecular orbital to contain more Fe than Mo character, i.e., a dative  $\text{Fe} \rightarrow \text{M}$  bond. The primary Fe-H bonding MO contains more H than Fe character and is somewhat delocalized onto Mo. The W-H coupling in **1** could be viewed as having contribution from a direct interaction combined with a three- $\sigma$ -bond coupling.

(26) McNeil, E. A.; Scholer, F. R. *J. Am. Chem. Soc.* **1977**, *99*, 6243.

(27) Ernst, R. D.; Marks, T. J.; Ibers, J. A. *J. Am. Chem. Soc.* **1977**, *99*, 2090.

(28) (a) Hall, K. P.; Mingos, D. M. P. *Prog. Inorg. Chem.* **1984**, *32*, 237.

(b) Lauher, J. W., reported in ref 28a.

(29) Band deconvolution performed as described in ref 10.

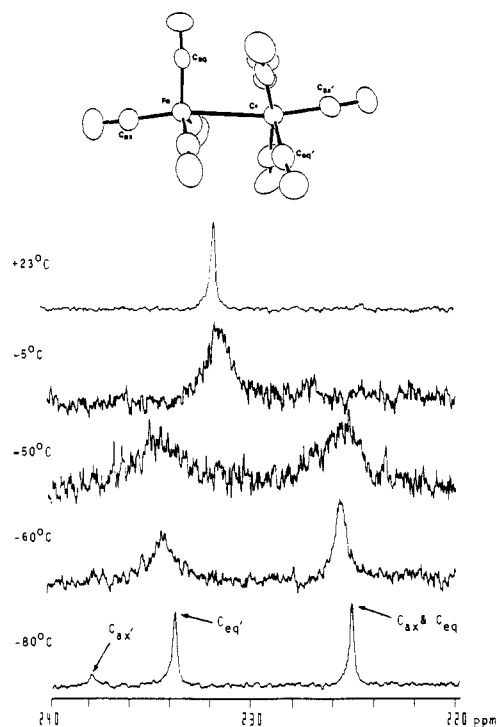


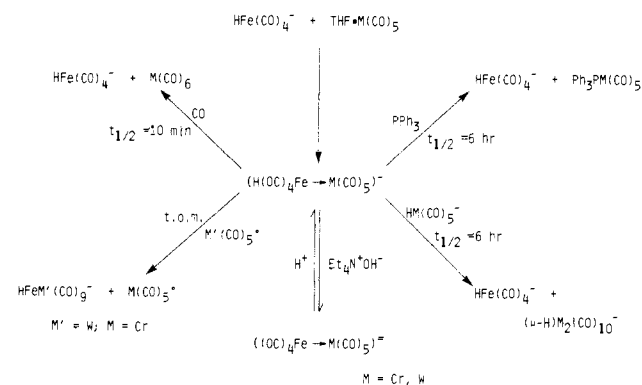
**Figure 6.** Temperature-dependent  $^{13}\text{C}$  NMR spectra for a solution of **4** in THF. At  $-80^\circ\text{C}$ , three resonances appear at 237.99, 233.92, and 225.29 ppm in a ratio of 1:4:4 corresponding to  $\text{Cr}(\text{CO})_{\text{ax}}$ ,  $\text{Cr}(\text{CO})_{\text{eq}}$ , and  $\text{Fe}(\text{CO})_{\text{ax,eq}}$ , respectively. The coalescence into one symmetrical peak at 231.57 ppm occurred at  $+23^\circ\text{C}$ .

*cis*- $\text{HW}(\text{CO})_4\text{PR}_3^-$  are in the range of 30 Hz, and the dimeric bridging hydride,  $\mu\text{-H}[\text{W}(\text{CO})_5][\text{W}(\text{CO})_4\text{P}(\text{OMe})_3]^-$ , has a  $J_{\text{P-H}}$  of 21 Hz.<sup>34</sup> The  $J_{\text{W-H}}$  couplings are also observed to be small (12–20 Hz) for  $\text{HFe}(\text{CO})_3\text{LW}(\text{CO})_5^-$  ( $\text{L} = \text{CO}, \text{PR}_3,$  and  $\text{P}(\text{OR})_3$ ). For comparison,  $J_{\text{W-H}}$  of  $\text{HW}(\text{CO})_5^-$  is 52.5 Hz,<sup>35</sup> of  $\mu\text{-HW}_2(\text{CO})_{10}^-$ , 42.0 Hz,<sup>32</sup> and of  $(\text{Ph}_3\text{PAu})(\text{H})\text{W}(\text{CO})_4$ , 37 Hz.<sup>36</sup> Again, a curious enhancement of  $J_{\text{W-H}}$  is observed for **9**,  $J_{\text{W-H}} = 33$  Hz, and for **11**,  $J_{\text{W-H}} = 28.5$  Hz.

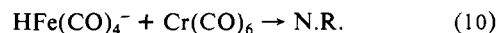
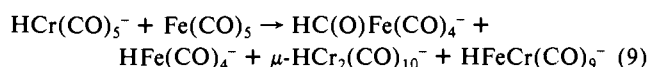
Selected  $^{13}\text{C}$  NMR data and assignments are given in Table II. For all anions studied, only one resonance is associated with carbonyl carbons of Fe, which are typically at ca. 220 ppm downfield from TMS. At higher field frequencies, the  $\text{C}_{\text{ax}}$  and  $\text{C}_{\text{eq}}$  resonances for the  $\text{W}(\text{CO})_5$  unit are observed for both  $\text{FeW}(\text{CO})_9^{2-}$  and  $\text{HFeW}(\text{CO})_9^-$ , at intensity ratios of ca. 1:4, and with appropriate  $^{183}\text{W}$ - $^{13}\text{C}$  satellites. In contrast, the resonances of carbons associated with Cr in  $\text{FeCr}(\text{CO})_9^{2-}$  are observed at field frequencies lower than those on Fe. The spectrum for  $\text{PPN}^+\text{HFeW}(\text{CO})_9^-$  in THF was invariant over the temperature range of  $-80$  to  $+50^\circ\text{C}$ , whereas those of the dianions  $\text{FeW}(\text{CO})_9^{2-}$  and  $\text{FeCr}(\text{CO})_9^{2-}$  were temperature-dependent. Complete coalescence of the  $\text{Fe}(\text{CO})_4$  resonance and the  $\text{M}(\text{CO})_5$  resonances occurs at  $+50^\circ\text{C}$  for  $\text{FeW}(\text{CO})_9^{2-}$  and at  $-30^\circ\text{C}$  for  $\text{FeCr}(\text{CO})_9^{2-}$ . For the latter, one sharp peak is seen at 231.6 ppm at  $+23^\circ$ , Figure 6. For the former, thermal decomposition occurs at the higher temperatures required to observe a sharp signal for the rapid exchange.

**Chemical Characterizations.** All chemical reactions disruptive of the dimer led to  $\text{HFe}(\text{CO})_4^-$  or  $\text{HFe}(\text{CO})_3\text{P}^-$  fragments. Even forcing conditions designed to drain off any  $\text{HW}(\text{CO})_5^-$  or  $\text{HW}(\text{CO})_4\text{P}^-$  species were unsuccessful in this regard.<sup>4</sup> All thermal degradations (vide supra) involving Fe–M bond cleavage were consistent with  $\text{HFe}(\text{CO})_4^-$  or  $\text{HFe}(\text{CO})_3\text{P}^-$  formation. That is, the Fe–H bond is less reactive (and presumably more stable)<sup>37</sup>

**Scheme I**

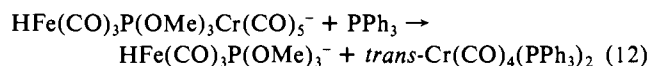
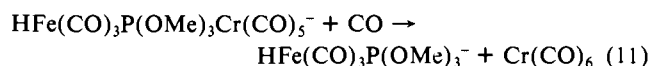


than group 6 M–H bonds in hydrido carbonyl anions.<sup>38</sup> This result is supported by all known hydride-transfer reactions from anionic metal hydrides. For example, eq 9 describes hydride transfer from  $\text{HCr}(\text{CO})_5^-$  to  $\text{Fe}(\text{CO})_5$  and represents in fact our initial observation of the  $\text{HFeCr}(\text{CO})_9^-$  species. The opposite reagent arrangement, eq 10, does not react.



Despite the implication of a simple thermal chemistry involving heterolytic  $\text{Fe} \rightarrow \text{M}$  bond cleavage, the  $\text{HFeM}(\text{CO})_9^-$  dimers possess more subtle chemical attributes. For example, reaction with CO, resulting in dimer cleavage, Scheme I, is very rapid and dependent on CO pressure, whereas that with  $\text{PPh}_3$  is slow when carried out under similar conditions. The half-lives given in Scheme I refer to 1:1 molar ratios of hydride to added ligand, CO or  $\text{PPh}_3$ . The group 6 hydrides,  $\text{HM}(\text{CO})_5^-$ , are also found to displace  $\text{HFe}(\text{CO})_4^-$ , generating the very stable  $\mu\text{-HM}_2(\text{CO})_{10}^-$  dimers. The rate of that reaction is comparable to the  $\text{PPh}_3$  displacement of  $\text{HFe}(\text{CO})_4^-$  under similar conditions.

Consistent with the shorter Fe–W bond length, the  $\text{HFe}(\text{CO})_3\text{P}(\text{OMe})_3\text{M}(\text{CO})_5^-$  dimers are much more resistant to disruption than are the all-CO analogues. Reactions with both CO and  $\text{PPh}_3$  (eq 11 and 12) are slow, requiring several days to come to completion when carried out in 1:1 molar ratio at room temperature. Kinetic studies of the reactions with  $\text{PPh}_3$  are under



way, and consistent with the observed product of disubstitution on Cr as indicated by eq 12, the rate-limiting step is indicated by activation parameters to be Cr–CO bond cleavage ( $\Delta H^\ddagger = 27.0$  kcal/mol;  $\Delta S^\ddagger = 3.8 \pm 2$  eu).<sup>39</sup> That is, dissociative CO/ $\text{PPh}_3$  substitution on the intact dimer precedes dimer disruption. For the  $\text{HFeW}(\text{CO})_9^-$  reaction with  $\text{PPh}_3$ , described in Scheme I, the products are monosubstituted  $\text{Ph}_3\text{PW}(\text{CO})_5$  and  $\text{HFe}(\text{CO})_4^-$ , the reaction is independent of  $[\text{PPh}_3]$  at  $[\text{PPh}_3]/[\text{HFeW}(\text{CO})_9^-]$  ratios greater than 5, and the rates are dependent on the dielectric constant of the solvent:  $\text{Me}_2\text{SO} > \text{CH}_3\text{CN} > (\text{CH}_3)_2\text{CO} > \text{THF} > \text{Et}_2\text{O}$ . Activation parameters for the latter reaction are  $\Delta H^\ddagger = 11 \pm 1.2$  kcal/mol and  $\Delta S^\ddagger = -48 \pm 6$  eu, suggesting a rate-determining configurational change or solvent reorientation preceding disruption of the dimer.

Scheme I also includes a metal-exchange reaction involving replacement of the  $\text{M}(\text{CO})_5$  unit. Addition of  $\text{THF}\cdot\text{W}(\text{CO})_5$  to  $\text{HFeCr}(\text{CO})_9^-$  results in a very rapid (time of mixing) group 6

(34) Slater, S. G.; Lusk, R.; Schumann, B.; Darenbourg, M. Y. *Organometallics* **1982**, *1*, 1662.

(35) Slater, S.; Darenbourg, M. Y. *J. Am. Chem. Soc.* **1981**, *103*, 5914.

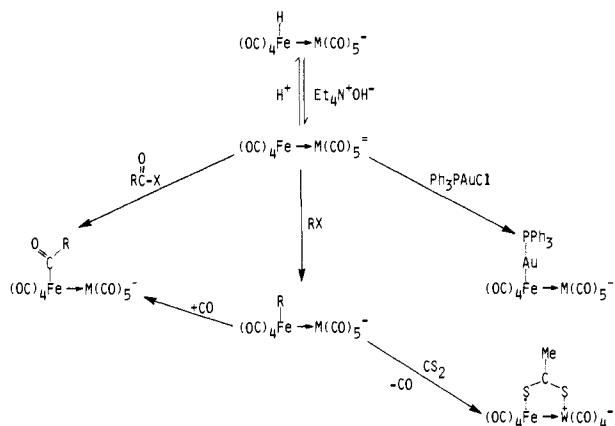
(36) Green, M.; Orpen, A. G.; Slater, I. D.; Stone, F. G. A. *J. Chem. Soc., Chem. Commun.* **1982**, 813.

(37) Elkind, J. L.; Armentrout, P. B., unpublished results.

(38) Kao, S. C.; Spillett, C. T.; Ash, C.; Lusk, R.; Park, Y. K.; Darenbourg, M. Y. *Organometallics* **1985**, *4*, 83.

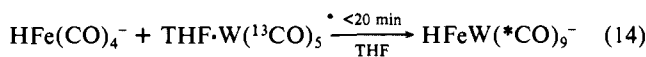
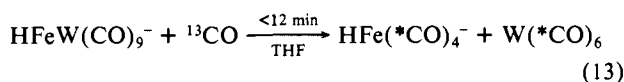
(39) Arndt, L. W.; Darenbourg, M. Y., unpublished results.

Scheme II



metal exchange. Similar metal exchanges have been attempted with other dimer anions. With  $\text{FeCr}(\text{CO})_9^{2-}$  and  $\text{THF}\cdot\text{W}(\text{CO})_5$ , only trace amounts of  $\text{FeW}(\text{CO})_9^{2-}$  were observed over several days of the reaction period. The reaction of  $\text{Ph}_3\text{PAuFeCr}(\text{CO})_9^-$  and  $\text{THF}\cdot\text{W}(\text{CO})_5$  yielded  $\text{Ph}_3\text{PAuFeW}(\text{CO})_9^-$  over the course of several hours. The C-13 label was scrambled into both components of the dimer.

Our preliminary report of the properties of  $\text{HFeW}(\text{CO})_9^-$  included both inter- and intramolecular CO lability. The reaction of  $\text{HFeW}(\text{CO})_9^-$  with  $^{13}\text{CO}$  split the dimer; however, C-13 label was incorporated into both monomeric products (eq 13). Since



\* = mixture of C-12 and C-13

neither product,  $\text{HFe}(\text{CO})_4^-$  or  $\text{W}(\text{CO})_6$ , is capable of such rapid CO exchange, we concluded that incorporation of labeled CO into the dimer preceded disruption. Intramolecular CO exchange was indicated in an experiment described by eq 14. Within the time required to obtain a  $^{13}\text{C}$  NMR spectrum, complete scrambling had occurred. Since, however, the CO's on Fe are clearly distinguishable from those on W in the NMR, up to 80 °C, the site exchange is slower than the NMR experiment time frame.

**Deprotonation Reactions.** Reagents such as  $\text{BuLi}$  readily remove  $\text{H}^+$  from  $\text{HFe}(\text{CO})_4^-$  as well as  $\text{HFeM}(\text{CO})_9^-$ . Potassium methoxide, solubilized with dibenzo-18-crown-6 rapidly and indiscriminately deprotonated  $\text{HFe}(\text{CO})_4^-$ , **1**, and **2**; it did not, however, react with *trans*- $\text{HFe}(\text{CO})_3\text{P}(\text{OMe})_3^-$ . Sodium hydroxide will not deprotonate  $\text{HFe}(\text{CO})_4^-$  but will deprotonate **1**, **2**, and **3**. The acidities of the hydrides vary as follows:  $\text{HFeW}(\text{CO})_9^-$ ,  $\text{HFeCr}(\text{CO})_9^- > \text{HFe}(\text{CO})_4^- \gg \text{HFe}(\text{CO})_3\text{P}(\text{OMe})_3^-$ .

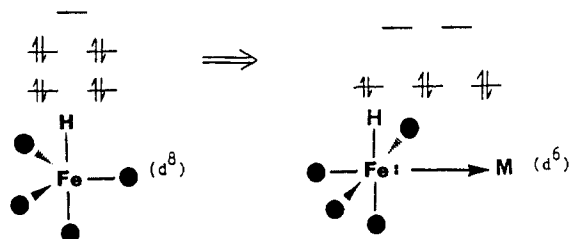
**$\text{MFe}(\text{CO})_9^{2-}$  Dianion.** The dianion which results from deprotonation of the hydride is more resistant to dimer disruption than is the hydride precursor. It is highly reactive with  $\text{O}_2$ ,  $\text{H}_2\text{O}$ , and electrophiles such as  $\text{Ph}_3\text{PAuCl}$  (vide supra),  $\text{PPh}_2\text{Cl}$ ,  $\text{RX}$ , and  $\text{RC}(\text{O})\text{X}$ . In all cases, the electrophiles add to the iron center, generating the mixed metal derivatives indicated in Scheme II.<sup>40</sup> Preliminary results on the organic halide derivatives suggest that the alkyl migration is greatly enhanced over the analogous Collman-type reagent derivatives.<sup>41</sup> Additionally, the  $\text{MeFeW}(\text{CO})_9^{2-}$

(40) We have at the time of this writing been unable to determine whether the  $\text{Ph}_2\text{P}$  derivative is to be formulated as  $\text{Ph}_2\text{PFeW}(\text{CO})_9^-$  or  $\text{Ph}_2\text{PFeW}(\text{CO})_8^{2-}$ .

$(\text{CO})_9^-$  anion reacts with  $\text{CO}_2$  and  $\text{CS}_2$ , generating in the latter case a very stable binuclear insertion product formulated as in Scheme II. A complete report of the reactivity of the heterobimetallic alkyl derivatives is in preparation.<sup>42</sup>

### Conclusions and Comments

A simple synthetic approach had led to a series of anionic complexes containing the functionalities of a polar metal-metal bond as well as an active metal hydride. The hydride is attached to the more electronegative metal, Fe, and there is no evidence at this time of its ever being transferred to the group 6 metal carbonyl unit. The ligation of  $\text{HFe}(\text{CO})_4^-$  to  $\text{M}(\text{CO})_5^0$  through Fe rather than through the hydride is rationalized by the formal achievement of a favored  $d^6$ , six-coordinate environment. Such



Fe-based nucleophilicity is preceded by the synthetic chemistry of  $\text{Fe}(\text{CO})_4^{2-}$ ,  $\text{HFe}(\text{CO})_4^-$ , and  $\text{RFe}(\text{CO})_4^-$  derivatives.<sup>43</sup> It is further supported by ion-pairing interactions in  $\text{Li}^+$  and  $\text{Na}^+$  salts of *trans*- $\text{HFe}(\text{CO})_3\text{PR}_3^-$  which show, in appropriate solvents, Fe...alkali cation contacts.<sup>10</sup> A similar orbital argument can be used to account for the hydride-based nucleophilicity of  $\text{HM}(\text{CO})_5^-$ , as in  $[(\text{OC})_5\text{M}-\text{H} \rightarrow \text{M}(\text{CO})_5]^-$ . Involvement of the group 6 metal in M-M bonding is disruptive of the  $d^6$ , octahedral coordination sphere.

Subtleties in reactivities of the various derivatives were not presaged by the X-ray structural data. There are no geometrical changes in the series ( $\text{HFeW}(\text{CO})_9^-$ ,  $\text{HFeCr}(\text{CO})_9^-$ ,  $\text{HFeW}(\text{CO})_8\text{P}(\text{OMe})_3^-$ , and  $\text{Ph}_3\text{PAuFeW}(\text{CO})_9^-$ ), and there is little variation in distances and angles. Yet properties such as dimer disruption or competitive ligand cleavage from the group 6 metal (i.e., loss of the metalloanion ligand vs. CO) are very sensitive to modifications of the anion.

The hydride ligand can be removed as  $\text{H}^+$ . It also appears to be a site of reactivity toward electrophiles. For example, exchange of the 16-electron transition-metal acceptor occurs rapidly with  $\text{HFeCr}(\text{CO})_9^-$  and much more slowly with  $\text{Ph}_3\text{PAuFeCr}(\text{CO})_9^-$ . The remarkable difference in reactivity of  $\text{HFeM}(\text{CO})_9^-$  with CO as compared to  $\text{PPh}_3$  may be attributed to the potential of the former to act as an electrophile. The reagents hold promise as good models for the study of bimetallic assisted reactions.

**Acknowledgment.** We express appreciation to the National Science Foundation (Grant No. CHE-8304162) for financial support of this work and to Maria M. Ludvig, Christine C. Kim, Kay A. Youngdahl, Y. K. Park, Carlton E. Ash, Patricia A. Tooley, and Edwar Shamshoum for assistance in portions of the work. Helpful discussion with Prof. M. B. Hall is also acknowledged.

**Supplementary Material Available:** Listings of the structure factor amplitudes for all structures (**1-4**) as well as corresponding ORTEP plots (84 pages). Ordering information is given on any current masthead page.

(41) Collman, J. P.; Finke, R. G.; Cawse, J. N.; Brauman, J. I. *J. Am. Chem. Soc.* **1978**, *100*, 4766.

(42) Arndt, L. W.; Janzen, C.; Youngdahl, K. A.; Darensbourg, M. Y., unpublished results.

(43) Collman, J. P. *Acc. Chem. Res.* **1975**, *8*, 342.